

## Measurements and FDTD Computations of the IEEE SCC 34 Spherical Bowl and Dipole Antenna

**Martin Siegbahn and Christer Törnevik**

Ericsson Radio Systems AB, S-164 80 Stockholm, Sweden

Phone: +46 8 7570811/7641235, Fax: +46 8 58531480

E-mail: martin.siegbahn@era-t.ericsson.se,  
christer.tornevik@era-t.ericsson.se

### *Summary*

*SAR and feedpoint impedance have been measured and FDTD computed for a spherical bowl and a  $\lambda/2$  dipole at 835 MHz according to procedures outlined by IEEE SCC 34, WG 1. Good agreement between measurement and FDTD computation was found both for the SAR distribution in the bowl and for the antenna feedpoint impedance.*

### **1 Introduction**

In order to evaluate the ability of the current state-of-the-art dosimetric nearfield measurement systems and computational tools to assess and predictate the electromagnetic fields close to low power radio transmitters the IEEE SCC 34 working group 1 has specified a number of so called canonical problems for benchmark testing. One of the problems involves a spherical glass bowl filled with brain simulating liquid and a wire dipole antenna which is placed below the bowl for inducing EM fields in the liquid [1]. The test consists of measurements or computations of the antenna feedpoint impedance as well as mapping of the specific absorption rate (SAR) in the liquid. This report describes the performed measurements and FDTD computations and the obtained results for this test at the EMF laboratory at Ericsson Radio Systems AB in Stockholm during May and June 1998.

### **2 Measurements**

The measurement procedures specify measurements of the SAR distribution from a  $\lambda/2$  wire dipole at 835 MHz in a spherical pyrex glass bowl filled with brain simulating liquid and the feedpoint impedance of this antenna when it is placed both symmetrically and asymmetrically below the bowl as shown in Fig. 1. The bowl has an outer diameter of  $224 \pm 0.5$  mm and a glass thickness  $5 \pm 0.5$  mm and the dipole has an overall length equal to 168 mm and a coaxial wire thickness of 3.6 mm. The dimensions of the dipole [2] are shown in Fig. 2. The opening in the spherical bowl is 170 mm in diameter ( $D_2$ ) and was chosen as to disturb the EM field distribution in the southern hemisphere as little as possible [1]. The liquid level was equal to 150 mm during all measurements.

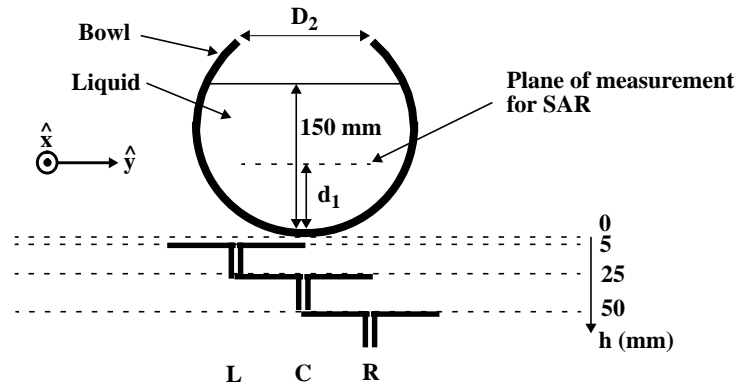


Figure 1. Three of the eleven different antenna positions below the spherical bowl. The separation between the bowl and the antenna is measured from the outer surface of both structures.

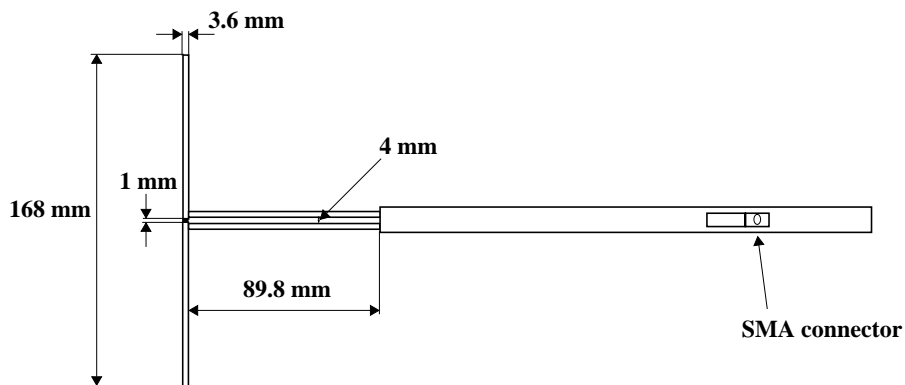


Figure 2. The 835 MHz  $\lambda/2$  dipole used in the measurements. The antenna was manufactured by Schmid & Partner Engineering AG with the model number D835V2 (S/N:401).

The measurement protocol states that the spherical bowl is filled with brain simulating liquid with a relative permittivity equal to 44.0 and a conductivity of 0.90 S/m. A recipe for mixing such a liquid was found by modifying a recipe giving similar parameters [3]; 41.5% water, 56.0% sugar, 1.4% salt, 1.0% HEC and 0.1% Preventol-7. The electrical parameters for this liquid were measured with a HP87050B dielectric probe kit and found to be at 835 MHz  $\epsilon_r=42.9\pm5\%$  and  $\sigma=0.90\pm10\%$  S/m [4].

Fig. 3 shows the laboratory setup for the measurements. A metal tripod holds the antenna and in order to properly position the antenna and the bowl a special fiberglass table with a 200 mm hole in the upper surface had to be fabricated. The distance between the antenna and the bowl was determined by use of a vernier calliper and the overall alignment by a water level.

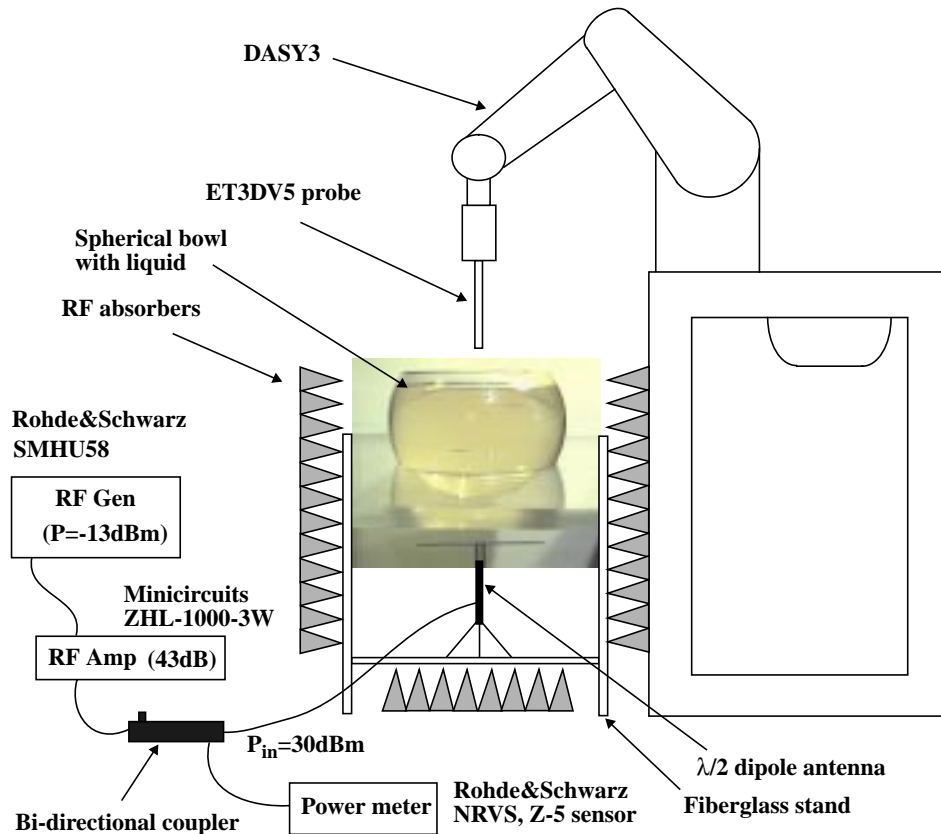


Figure 3. The laboratory setup for the IEEE SCC 34 spherical bowl and dipole experiment.

The dosimetric nearfield measurement system used for the SAR measurements was the DASYS3 [5] from Schmid & Partner Engineering AG with the isotropic E-field probe ET3DV5 [6]. The probe correction factor used for all SAR measurements in the bowl was equal to 6.1.

The impedance of the 835 MHz  $\lambda/2$  dipole was measured with a HP8752C network analyzer when the antenna was placed in all eleven different positions with respect to the bowl; as centered at distances (denoted  $h$ ) 5, 25 and 50 mm below the outer south pole and translated on both sides so that alternatively one of the antenna tips will be placed under the south pole at the same distances plus 0 mm. The SAR in the bowl was measured at the axis of symmetry for five of the positions; in the centered position with  $h=5, 25$  and 50 mm and left/right translated with  $h=0$  mm. Complete SAR scanning in horizontal planes at height  $d_1$  from the inner south pole was performed for the centered position at  $h=5$  mm and left/right position at  $h=0$  mm. The impedance measurements were conducted five times giving eleven values for each series and the SAR measurements were repeated three times. The complete SAR scanning was performed once for every measurement series but each axis of symmetry measurement was repeated five times in sequence in order to give reliable results.

### 3 FDTD computations

The spherical bowl and the dipole were modeled in a cubical FDTD grid [7] with grid step equal to 2.5 mm, as shown in Fig. 4 and Fig. 5. This grid step was chosen as suitable for computing distances 5, 25 and 50 mm between the bowl and the antenna but also giving moderate modeling errors for the dimensions of both structures. Obviously, in order to have a symmetrical antenna, the length of the antenna model is always an odd number of cells and therefore the diameter of the bowl also has to be an odd number of cells if the antenna is to be placed in a true centered position below the bowl. This requires though that the antenna is modeled as a bar of cells rather than by a thin filament of FDTD components if the models are to be symmetrical also in the plane perpendicular to the antenna axis. However, when modeling the case with a asymmetrically positioned antenna the tip of the dipole is not possible to placed directly under the outer south pole but it will be a half grid step offset from this position.

The FDTD components in the glass-liquid boundary, i.e. on the inside of the bowl, were computed with the material parameters set equal to those for the liquid since the pyrex glass has a zero conductivity. In the 2.5 mm grid, the bowl has an outer diameter of 89 cells, i.e. 222.5 mm, and an inner diameter of 85 cells, i.e. 212.5 mm. The antenna is represented by two bars each 33 cells long with a one by one cell cross section giving an overall length, including the voltage source gap, of 67 cells or 167.5 mm.

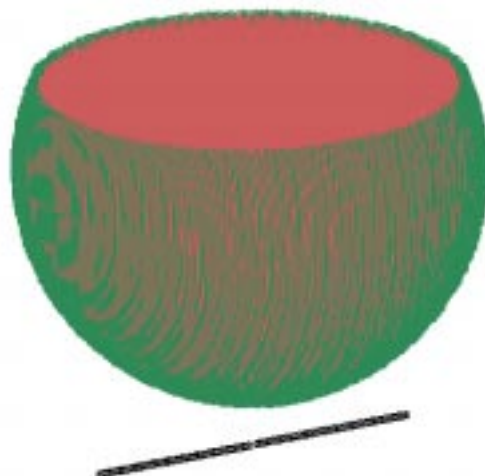


Figure 4. The FDTD models of the spherical bowl and the  $\lambda/2$  dipole. The dipole is placed as centered 25 mm below the outer south pole of the bowl.

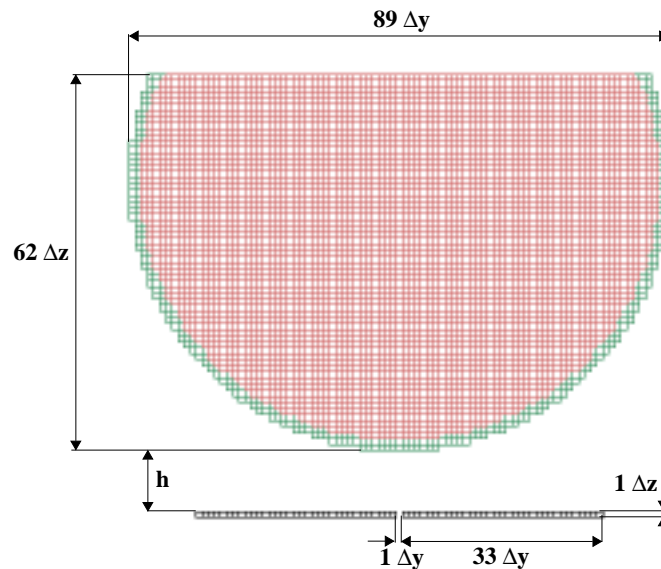


Figure 5. The dimensions of the FDTD models. The separation  $h$  between the bowl and the dipole, was 2, 10 and 20 cells corresponding to distances 5, 25 and 50 mm.

The bowl and the halfwave dipole were placed in the FDTD grid with a minimum distance to the Liao boundary of  $\lambda/3$  giving a total computational volume of  $165 \times 165 \times 165$  cells for the computations with the dipole in a centered position and  $165 \times 190 \times 165$  cells for the case when it was placed asymmetrically. The memory requirements for these grids were 127 and 146 Mbyte respectively in the XFDTD version 4.04 code [8] and on the 300 MHz Sun Ultra-30 computer the computational time was about 5h 15min.

## 4 Measurement and FDTD Results

### 4.1 Antenna feedpoint impedance

Table 1 summarizes the obtained measured and FDTD computed feedpoint impedance of the half-wave dipole antenna when it was positioned in the different positions. Note, the FDTD data for the left translated antenna is only a copy of the right side data since computations of this case will give close to identical values, which is of course due to the symmetry of the applied models.

Position	h(mm)	Measured Re(Z), mean value ( $\Omega$ )	Measured Im(Z), mean value ( $\Omega$ )	FDTD Re(Z) ( $\Omega$ )	FDTD Im (Z) ( $\Omega$ )
Centered	5	49.7	-4.6	48.9	-2.8
Centered	25	53.9	14.8	48.9	18.5
Centered	50	74.9	23.4	66.0	29.6
Right	0	104.6	91.4	178.6	159.2
Right	5	82.0	45.5	90.5	44.2
Right	25	75.1	24.6	75.1	23.8
Right	50	84.2	20.6	78.8	22.3
Left	0	105.1	89.9	178.6	159.2
Left	5	82.8	43.6	90.5	44.1
Left	25	76.6	22.7	75.1	23.8
Left	50	85.8	18.9	78.8	22.3

**Table 1** The measured and FDTD computed feedpoint impedance for the  $\lambda/2$  dipole at 835MHz.

The maximum differences between the measured right side and the left side values are 1.6  $\Omega$  for the resistance and 2.0  $\Omega$  for the reactance. The standard deviation for the measured resistance ranges from 0.4 to 12.9  $\Omega$  and for the measured reactance 0.4 to 2.8  $\Omega$ . The maximum difference between the measured mean and the FDTD computed impedance for the centered position is of the order 6 to 9  $\Omega$ .

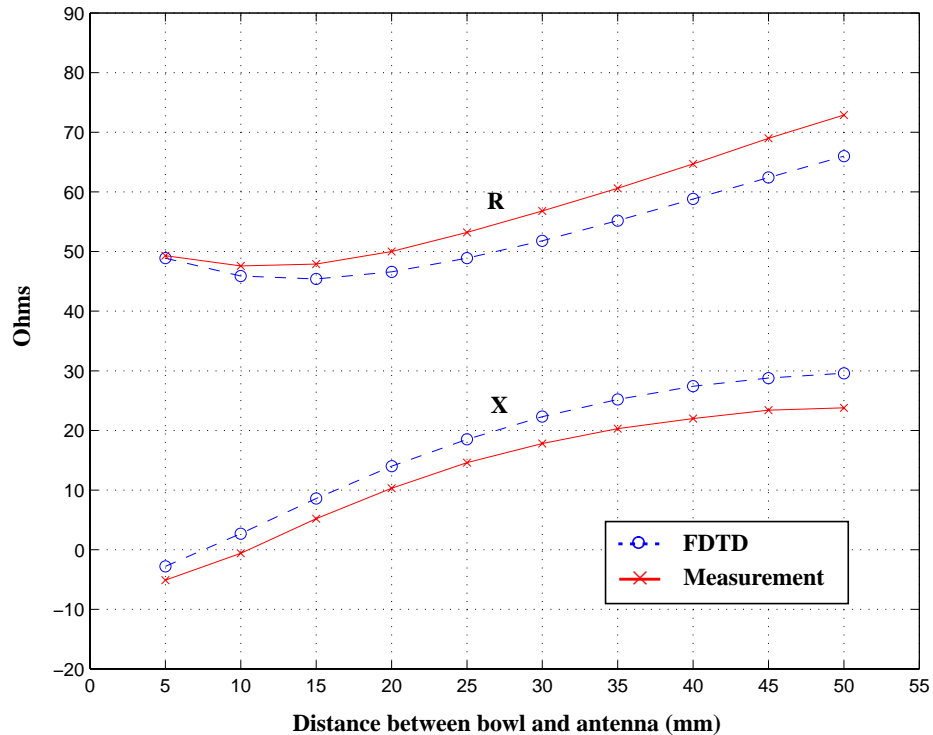


Figure 6. FDTD computed vs. measured dipole feedpoint impedance for centered antenna position. The measured impedance displayed are only based on one series of values.

An additional series of impedance measurements were performed for the case when the dipole was placed symmetrically below the bowl. The impedance was measured for distances  $h=5$  to 55 mm in 5 mm steps in order to investigate the overall antenna-bowl separation dependence of the feedpoint impedance. Corresponding FDTD computations were also carried out and the results are shown in Fig. 6. The agreement between measurement and FDTD calculation is very good and the mean difference is only about  $4 \Omega$  for both the resistance and the reactance. Obviously, the selected FDTD models seem suitable for computing the feedpoint impedance even though they are, in certain aspects, somewhat coarse.

## 4.2 SAR results

In order to properly compare the measured and the FDTD computed SAR distributions in the bowl, the FDTD values had to be calculated by averaging over several computational cells and E-field components [9]. All SAR values were normalized to 1W of radiated power.

### 4.2.1 SAR on the axis of symmetry

The measured and the FDTD computed local SAR on the axis of symmetry in the spherical bowl when the antenna was placed symmetrically below it is shown in Fig. 7. The agreement between measurement and FDTD computation is very good for all distances between the bowl and the antenna. The peak local SAR is, of course, located at the inner surface of the bowl and falls off quite rapidly with increasing height/distance from the inner surface. The measured SAR decreases somewhat faster though than the FDTD data close to the inner south pole. However, small deviations in probe positioning in this area lead to large variations in measured SAR which is shown by the standard deviation for these measurement points, about 1.7 W/kg for the distance 2.7 mm when  $h$  was equal to 5mm.

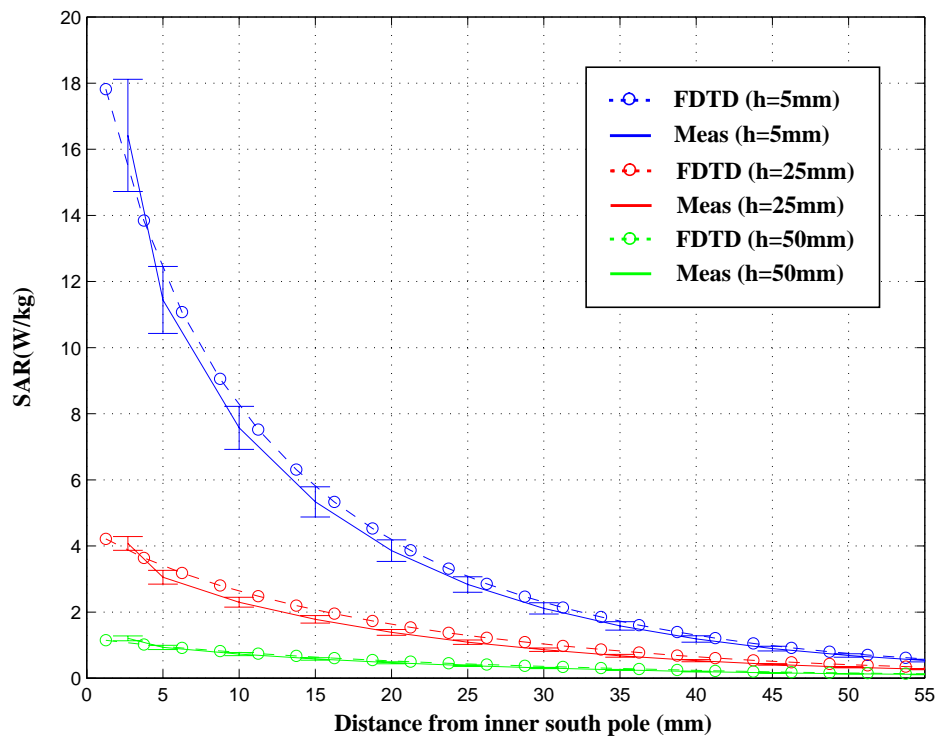
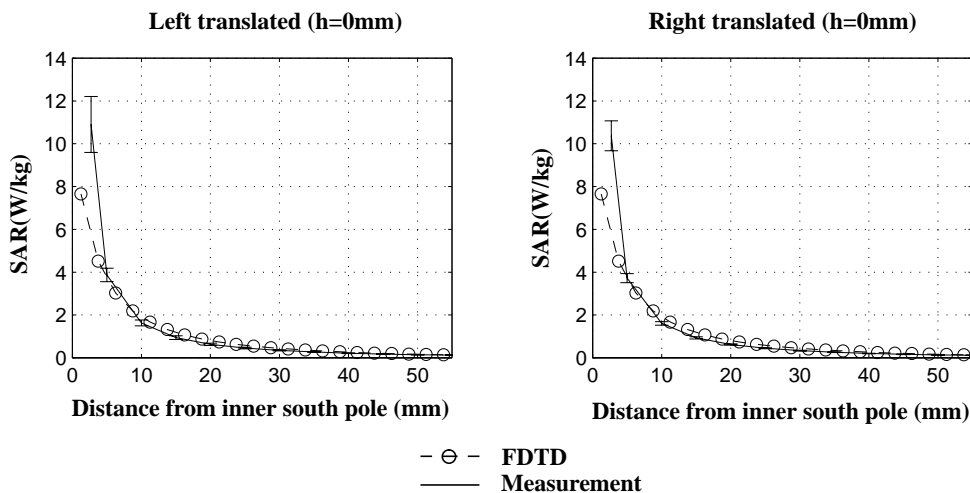


Figure 7. FDTD computed vs. measured SAR on the axis of symmetry for the spherical bowl. The dipole was placed as centered 5, 25 and 50 mm below the outer south pole.

The SAR decrease due to increased separation between the bowl and the dipole antenna is also clearly understandable and an increase in  $h$  from 5 mm to 50 mm decreases the maximum SAR almost by a factor of 10 both in the measurements and in the FDTD computations. The mean difference between the measurement and the FDTD data is 0.2 W/kg for  $h=5$  mm, 0.1 W/kg for  $h=25$  mm and only 0.03 W/kg for  $h=50$ mm.

For the cases when the dipole antenna was translated to the left and right side of the bowl the measured and the FDTD computed local SAR on the axis of symmetry for the bowl are shown in Fig. 8. The agreement between measurement and computation is not as good as when the dipole antenna was placed in a centered position. Here, the FDTD computed SAR close to the surface is lower than the measured value. The maximum difference between the two data sets is for the left translated position about 5.4 W/kg close to the inner surface but the overall mean difference is only of the order 0.3 W/kg. For the right translated case the corresponding differences are 4.7 W/kg and 0.3 W/kg. However, the agreement between the two measurement data sets is rather good though which indicates good positioning and alignment of the laboratory setup.



**Figure 8.** The measured and the FDTD computed SAR on the axis of symmetry for the spherical bowl. The half-wave dipole antenna was placed 0 mm below the outer south pole and translated to the left and right side.

#### 4.2.2 SAR in horizontal planes at heights $d_1$ above the inner south pole

Local SAR measured and computed in horizontal planes at heights  $d_1=30$  mm and  $d_1=50$  mm from the inner south pole for the symmetrically positioned antenna at  $h=5$  mm are shown in Fig. 9 and 10. The agreement between the measured and the FDTD computed SAR is quite good both in terms of absolute value and shape. The mean difference is only of the order 0.1 W/kg for both planes. At the height  $d_1=30$  mm the axis of the antenna is clearly visible as a ridge in the SAR distribution along the y-axis but at  $d_1=50$  mm the distribution is more or less symmetrical around the maximum value located at the center of the plane.

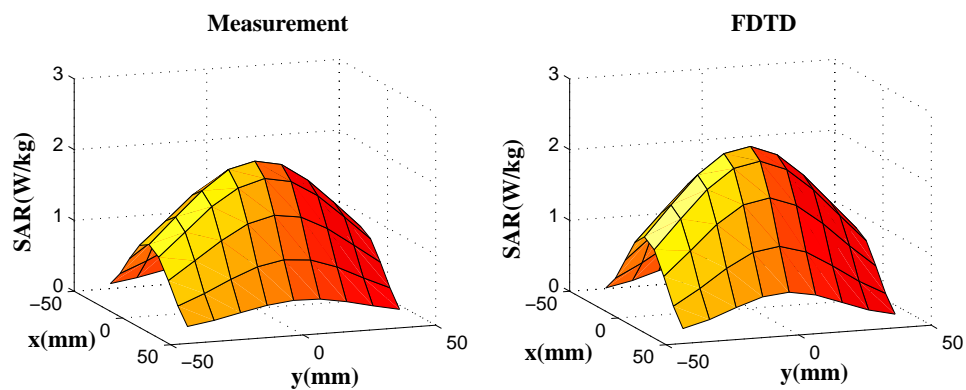


Figure 9. Local SAR in the plane  $d_1=30$  mm for the center antenna position at  $h=5$  mm. The maximum and the mean differences between the measurement and the FDTD computation are 0.3 W/kg and 0.1 W/kg.

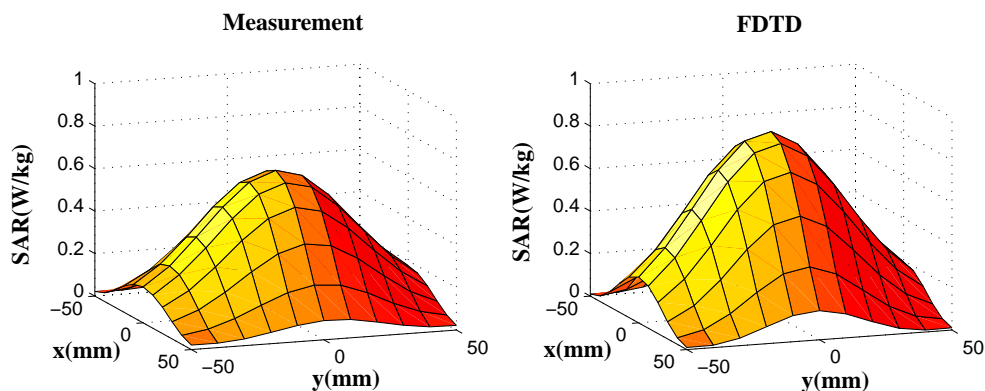


Figure 10. Local SAR in the plane  $d_1=50$  mm for the center antenna position at  $h=5$  mm. The maximum and the mean differences between the measurement and the FDTD results are 0.2 W/kg and 0.06 W/kg.

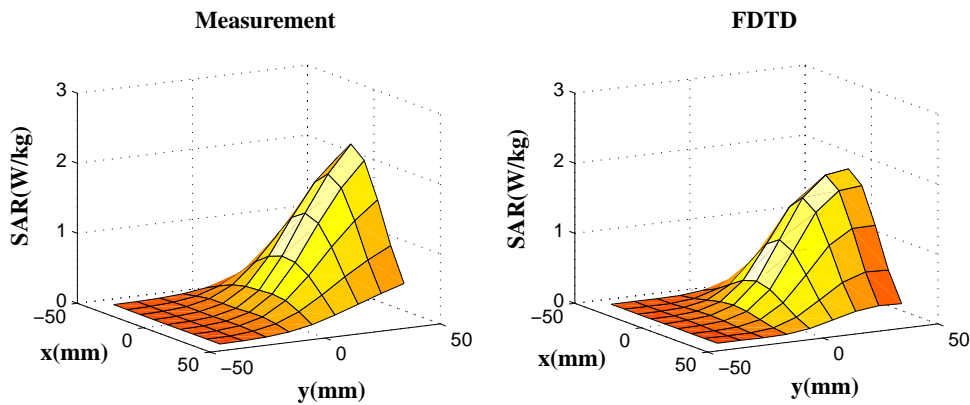


Figure 11. Local SAR in the plane  $d_1=50$  mm for the right translated antenna position at  $h=0$  mm. The maximum and the mean differences between the measurement and the FDTD computation are 0.4 W/kg and 0.1 W/kg.

In Fig. 11, the SAR distribution at  $d_1=30$  mm for the right translated antenna position are shown. The maximum value of this distribution is located at the right side of the plane and here there are some differences between measurement and FDTD computation. This is probably due to the fact that the tip of the antenna in the FDTD model is not possible to perfectly position at the outer south pole but is located half a grid step to the right of the pole.

## 5 Conclusions and Future work

Measurements and corresponding FDTD computations have been performed for the IEEE SCC 34 spherical bowl and dipole benchmark test with good agreement in the obtained results both in terms of the antenna feedpoint impedance and the SAR distribution in the bowl. The mean difference between measured and FDTD calculated impedance was found to be around 6-9  $\Omega$  and the mean difference between the measured and the FDTD computed SAR in the bowl was of the order 0.05-0.4 W/kg. However, the uncertainties and errors affecting the measurement and the FDTD results both in terms of SAR and impedance have not yet been finally calculated but will be included and described in the next revision of this document.

## 6 References

- [1] IEEE SCC 34, WG 1, "Spherical Phantom Experimental Protocol", 2nd Draft, 1998.
- [2] Thomas Schmid and Katja Pokovic, "FCC Benchmark Dipole B", Swiss Federal Institute of Technology Zurich, 8096 Zurich, Switzerland.
- [3] G. Hartsgrrove, A. Kraszewski and A. Surowiec, "Simulated biological materials for electromagnetic radiation absorption studies", *Bioelectromagnetics*, vol. 8, pp. 29-36, 1997.
- [4] Hewlett-Packard Company, "HP85070B Dielectric Probe Kit User's manual", HP part number 85070-90009, 1993.
- [5] Thomas Schmid, Oliver Egger, Niels Kuster, "Automated E-field scanning system for dosimetric assessments", *IEEE transactions on Microwave Theory and Techniques*, vol. 44, pp. 105-113, January 1996.
- [6] Klaus Meier, Michael Burkhardt, Thomas Schmid and Niels Kuster, "Broadband calibration of E-field probes in lossy media", *IEEE transactions on Microwave Theory and Techniques*, vol. 44, no. 10, pp. 1954-1962, October 1996.
- [7] Karl S. Kunz, Raymond J. Luebbers, "The Finite Difference Time Domain Method for Electromagnetics", CRC Press, 1993.
- [8] Remcom Inc., "User's Manual for XFDTD the X-Window Finite Difference Time Domain Graphical User Interface for Electromagnetic Calculations", Version 4.04, October 1997.
- [9] K. Caputa, M. Okoniewski and Maria A. Stuchly, "An Algorithm for Computations of the Power Deposition in Human Tissue with the FDTD Method", Proceedings of the USNC/URSI National Radio Science Meeting 1998, Atlanta, Georgia, U.S, June 21-26 1998, pp. 197.